Mon. Not. R. Astron. Soc. **000**, 1–15 (2002) Printed 5 February 2008 (MN LATEX style file v2.2)

Finding structures in photometric redshift galaxy surveys: An extended friends-of-friends algorithm

C. S. Botzler,[1] J. Snigula,[1] R. Bender,[1,2] U. Hopp[1]
[1]*Universitäts-Sternwarte München, Scheinerstr. 1, D-81679 München, Germany*
[2]*Max-Planck-Institut für extraterrestrische Physik, Giessenbachstr., D-85748 Garching, Germany*

Accepted –; Received –;

ABSTRACT
We present a modified version of the friends-of-friends (FOF) structure finding algorithm (Huchra & Geller 1982), designed specifically to locate groups or clusters of galaxies in photometric redshift datasets. The main objective of this paper is to show that this extended friends-of-friends (hereafter EXT-FOF) algorithm yields results almost identical to the original FOF, if applied to a spectroscopic redshift dataset, and a rather conservative catalogue of structures, in case of a dataset with simulated photometric redshifts. Therefore, we create group catalogues for the first Center for Astrophysics Redshift Survey (CFA1; Huchra et al. 1983), as well as for the Las Campanas Redshift Survey (LCRS; Shectman et al. 1996), both of which being spectroscopic surveys, using FOF-algorithms. We then apply our new algorithm to said surveys and compare the resulting structure catalogue. Furthermore, we bestow simulated photometric redshifts on the LCRS galaxies, and use the EXT-FOF to detect structures, that we compare in size and composition to the ones found in the original, spectroscopic dataset. We will show that the properties of this modified algorithm are well understood and that it is suited for finding structures in photometric datasets. This is the first paper in a series of papers, dealing with the application of our new cluster finding algorithm to various photometric redshift galaxy surveys.

Key words: catalogues – galaxies: clusters: general – methods: analytical – data analysis

1 INTRODUCTION

Optical and near-IR galaxy surveys, and especially the groups and clusters of galaxies found therein, have been playing an important role in our understanding of structure formation and cosmology. As has been shown by Press & Schechter (1974), Peebles (1993), and Eke et al. (1996), among others, the evolution of the mass-function of groups and clusters of galaxies is highly sensitive to cosmological parameters, the type of dark matter and the biasing of dark against baryonic matter. Thus, comparison of the mass-function predicted by semi-analytic structure formation models, like the Press-Schechter formalism (Press & Schechter 1974), or N-body simulations with the observed mass-function yields strong constraints on structure formation scenarios and the cosmological paradigm (Bahcall & Cen 1992; Ueda et al. 1993; Jing & Fang 1994; Bahcall et al. 1997; Bode et al. 2001). Finding large-scale structures in galaxy surveys is also an important step in examining the evolution of galactic properties, like the luminosity function, in high- and low-density environments (Trentham 1998; de Propris et al. 1999; Drory et al. 2001a; Fried et al. 2001; Postman et al. 2001).

With the development of the photometric redshift determination techniques (Baum 1962; Koo 1985; Brunner et al. 1999; Fernández-Soto et al. 1999; Benítez 2000; Bender et al. 2001), approximate redshifts became available for all galaxies in a photometric multi-band survey, without having to do time-consuming spectroscopic follow-up observations. This type of galaxy survey is increasing in popularity. The list of surveys using photometric redshift determination includes the Hubble Deep Fields (HDF) North and South (Williams et al. 1996, 2000), the Las Campanas Infrared Survey (LCIR; Marzke et al. 1999, McCarthy et al. 2001a, b), the Calar Alto Deep Imaging Survey (CADIS; Wolf et al. 2001a), the Classifying Objects by Medium-Band Observations Survey (COMBO-17; Wolf et al. 2001b), the Munich Near-IR Cluster Survey (MUNICS; Drory et al. 2001b), and the Fors Deep Field (FDF; Heidt et al. 2003). However, photometrically determined redshifts possess larger errors than spectroscopically determined ones. The accuracy of the photometric redshift determination is typically worse than the spectroscopic one by more than two orders of magnitude. Thus, the photometric redshift errors correspond to roughly 50 times the typical velocity dispersion of bound structures, like galaxy groups or clusters.

The actual identification of groups or clusters of galaxies, either in an observed or simulated catalogue, is a non-trivial enterprise. A reliable detection of large-scale structures in an observed galaxy catalogue is even more complicated if the galaxies have only photometric redshifts or, even worse, none at all. Up to now, many different techniques have been created for the purpose of structure

finding. All of them have their advantages and disadvantages and are constructed to fit the specific features of their surveys, like the wavelength of the observed radiation, or whether redshifts were determined for all objects, and if so, what type of redshift determination was used. Giving a complete list of all types of structure finding techniques applied to optical and near-IR data, and their individual implementations would exceed the scope of this paper. However, we give a brief overview over the more important ones and their working principles, to better place our work in the context of structure finding.

The pioneering work in this field was achieved by Abell (1958), followed by Abell et al. (1989), Lidman & Peterson (1996), and Dalton et al. (1997), amongst others. Their counts-in-cells method looks for surface density enhancements in circular apertures of fixed physical radius. A modification to this approach was used by Zwicky et al. (1968), Turner & Gott (1976), Couch et al. (1991), and Plionis et al. (1991), who searched for surface density enhancements by method of isopleth-contours. Another rather famous method is the hierarchical clustering technique (Materne 1978; Tully 1980; Hopp & Materne 1985; Tully 1987; Gourgoulhon et al. 1992). It identifies structures on the basis of optimising typical cluster or group properties, such as spatial separation or luminosity density, by combining individual galaxies into groups, with the advantage of delivering a list of local concentrations within the groups, and superstructures at given values of the property that is to be optimised. One of the more recently developed methods is the matched or generalised likelihood filter (Postman et al. 1996; Schuecker & Boehringer 1998; Kepner et al. 1999; Lobo et al. 2000). On the basis of Bayesian probability theory, the galaxy catalogue is convolved with a set of models, the filter, describing typical cluster properties, like the radial profile or the luminosity function, thus determining the likelihood of having clusters with given positions and richnesses in the input dataset. Voronoi tessellation has also been used as a means of detecting large-scale structures (Ramella et al. 2001; Kim et al. 2002). In this case, a unique plane or volume partition of the galaxy distribution is done, yielding a measure for the local densities, thus enabling identification of groups or clusters as significantly overdense regions. Techniques looking for spherical density enhancements have been used by Lacey & Cole (1994) and Cole & Lacey (1996). Some more exceptional approaches are the wavelet decomposition (Slezak et al. 1990; Paredes et al. 1995), the HOP algorithm (Eisenstein & Hut 1998), the cluster red sequence approach (Gladders & Yee 2000), or the cut-and-enhance method (Goto et al. 2002).

Probably the most extensively used structure finding algorithm is the friends-of-friends technique or percolation algorithm. This method looks for number density enhancements in three dimensions by searching for galaxy pairs, that are closer to one another than a given cut-off separation. Consequently, the friends-of-friends does not suffer a bias as far as the radial profile, or luminosity function are concerned, as is for example the case for the matched filter technique. Up to now, the friends-of-friends (FOF) approach has only been applied to spectroscopic redshift surveys (Huchra & Geller 1982; Geller & Huchra 1983; Ramella et al. 1989, 1997; Trasarti-Battistoni 1998; Giuricin et al. 2000; Merchán et al. 2000; Tucker et al. 2000; Ramella et al. 2002), or N-body simulations (Davis et al. 1985; Efstathiou et al. 1988; Lacey & Cole 1994; Cole & Lacey 1996; Valageas et al. 2000). In the first case, the spectroscopic redshift is a combination of the Hubble expansion and the peculiar velocity of the galaxy, thus being a very good estimate of the true distance to the galaxy. In the second case, the exact position in three-dimensional space is known. Applying this algorithm to a galaxy catalogue with photometric redshifts constitutes a problem, due to the less than perfect distance information. If the redshift errors are not taken into account, the resulting structure catalogue will contain highly unphysical groups and clusters. If the errors are taken into account, yet the algorithm itself is not changed, the procedure yields structures, that are extremely elongated in redshift ($\Delta z \sim 1$). Thus it proves necessary to develop a new type of FOF algorithm, the extended friends-of-friends, for photometric redshift datasets, that includes the redshift error information and at the same time cuts down on unrealistically elongated structures.

Section 2 gives a brief overview of the original FOF technique of Huchra & Geller (1982) and introduces the EXT-FOF algorithm. The following two sections prove, that in case of galaxy catalogues with spectroscopically determined redshifts, both algorithms yield almost identical group catalogues. In Section 3, both friends-of-friends algorithms are applied to the spectroscopic CFA1 survey, following the recipe given by Geller & Huchra (1983). The resulting group catalogues are compared on an object-to-object basis and the deviations are explained. The same is done for the LCRS in Section 4, following the approach of Tucker et al. (2000). In order to show that our EXT-FOF technique provides a conservative group and cluster catalogue for photometric galaxy surveys, we simulate photometric redshifts for the LCRS galaxies in Section 5. We then apply our EXT-FOF to this new dataset and compare the detected structures to the ones found with the EXT-FOF algorithm in the original, spectroscopic dataset.

This paper is the first in a series, dealing with the search for large-scale structures, like groups and clusters of galaxies, in photometric redshift datasets. In the next paper, we will apply our new cluster finding technique to MUNICS and test the plausibility of the found structures, using colour-magnitude diagrams, Voronoi tessellations, and a likelihood approach. The same will be performed for the FDF galaxy catalogue in our third paper.

2 FRIENDS-OF-FRIENDS (FOF) ALGORITHMS

The friends-of-friends algorithm, that was invented by Huchra & Geller (1982), is one of the most frequently used cluster finding techniques. It was designed to find number overdensities in spectroscopic galaxy surveys and has also been modified to look for structures in simulated galaxy datasets. The FOF approach is very straightforward and has no need for complicated cluster models. It looks for galaxy pairs, that are closer to one another than a given cut-off separation. One of the resulting advantages is its insensitivity to cluster shape. However, like most of the other structure finding techniques, it has the drawback of being rather slow in its application. Changing the cut-off parameters requires a new run of the procedure, which makes the optimisation of the cut-off values time-consuming.

2.1 The Huchra & Geller friends-of-friends algorithm

The original FOF algorithm was created to look for groups and clusters of galaxies in the magnitude-limited CFA1 redshift survey (Huchra & Geller 1982; Huchra et al. 1983; Geller & Huchra 1983). It makes use of three basic pieces of information, the positions of the galaxies in right ascension and declination, and their spectroscopic redshifts.

A slightly modified version of the algorithm's flow chart given

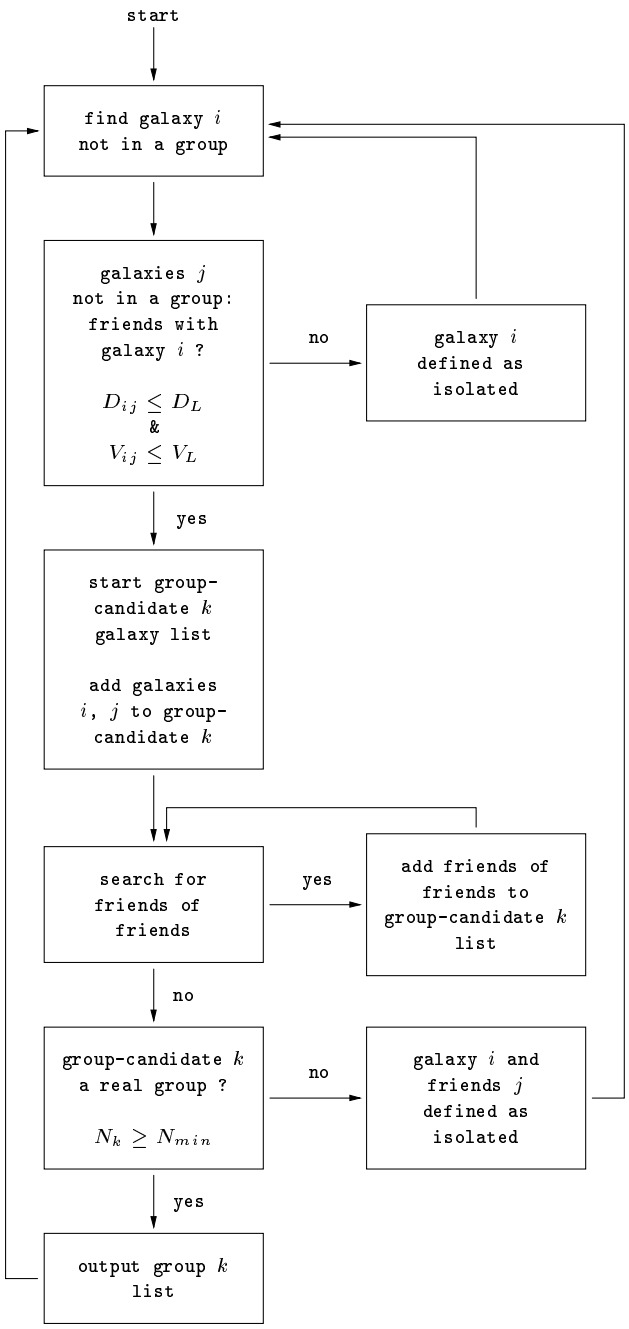

Figure 1. Flow chart for the Huchra & Geller friends-of-friends algorithm

by Huchra & Geller (1982) is shown in Fig. 1. First, an object i from the galaxy catalogue, that has not yet been assigned to any group, is chosen. Then friends j of that galaxy are searched for. They have to fulfill two criteria. Their projected separation D_{ij} from the first galaxy has to be less than a critical value D_L:

$$D_{ij} := 2 \sin \frac{\theta_{ij}}{2} \frac{\overline{V}}{H_0} \leq D_L, \tag{1}$$

where θ_{ij} is the angular separation between galaxies i and j, H_0 is the Hubble constant, and $\overline{V}$ is the mean velocity of the galaxy pair:

$$\overline{V} = \frac{v_i + v_j}{2}, \tag{2}$$

v_i and v_j being the velocities of the individual galaxies. Furthermore, their separation V_{ij} in velocity-space has to be less than a second critical value V_L:

$$V_{ij} := |v_i - v_j| \leq V_L. \tag{3}$$

If there are no friends for galaxy i, it is called an isolated object and removed from the catalogue of possible cluster members. If friends are found for galaxy i, a list for group-candidate k is initiated, containing galaxy i and all of its friends j, that fulfill eqs. (1) and (3). The search for friends is extended to the surroundings of the galaxies j. All friends found are once more added to the group-candidate k. This is done until no further friends of friends can be detected. The group-candidate k is called a real group, if the number N_k of its members exceeds the limit N_{min}:

$$N_k \geq N_{min}. \tag{4}$$

If this is not the case, all members of said group-candidate are removed from the catalogue. The next galaxy from the catalogue is then taken and its surroundings are searched for friends.

As can be seen easily, this algorithm is commutative and yields reproducible results, which are very important features for any structure finding technique.

The choice for the linking parameters D_L and V_L depends on the properties of the input galaxy dataset. In principle, both parameters can be chosen to remain either fixed or to vary with redshift. The minimum group size limit N_{min} is usually set to 3. Thus only galaxy pairs are excluded from the final group catalogue.

2.2 The extended friends-of-friends algorithm

Due to the relatively large errors in the photometric redshifts, the friends-of-friends algorithm cannot be used for this type of dataset without some modifications. If the photometric redshift errors are not taken into account, a large fraction of the resulting groups and clusters are not physically bound objects. While the linking velocity V_L of the original FOF usually corresponds roughly to typical cluster velocity dispersions, photometric redshift errors are normally larger by a factor of 50. This implies that the deviation between the measured and the true distance to a galaxy might be off by about 50 times the linking velocity. Identification of these galaxies as group members is impossible with the original FOF technique. On the other hand, galaxies, whose true positions on the velocity axis are deviant by about 100 V_L, could be combined into groups. Simply including the redshift errors of the individual galaxies into the linking criteria does not solve this dilemma either. The resulting structures would get unreasonably extended in redshift. Allowing for the necessary large value in the linking velocity would enable huge chains of galaxies to be linked together by the FOF algorithm. Thus, a modified version of the FOF algorithm, the extended friends-of-friends or EXT-FOF, becomes necessary for photometric redshift galaxy surveys.

The EXT-FOF technique utilises the same informations as the original FOF, i.e. right ascensions, declinations and, in this case, photometric redshifts of the galaxies. Furthermore the individual redshift error of each galaxy is taken into account.

The algorithm itself consists of three parts: In its inner loop, the technique is almost identical to the Huchra & Geller method, with slightly altered linking conditions. The search for groups is done in various a priori redshift-slices, meaning only galaxies that are compatible with a given value of redshift are taken into account for cluster finding. This redshift-slicing constitutes the outer loop.

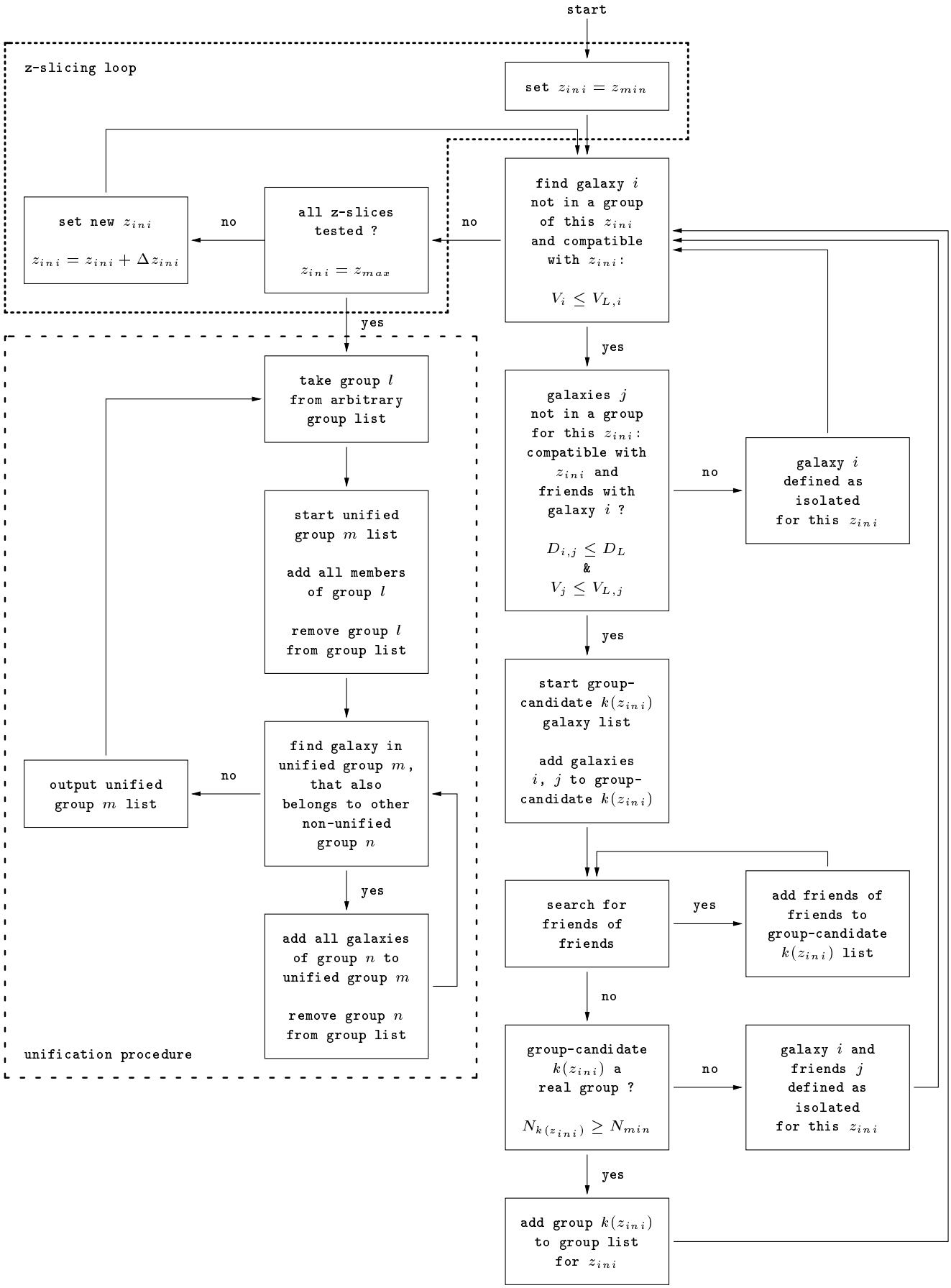

Figure 2. Flow chart for the extended friends-of-friends algorithm

As a result, there is a catalogue of structures for every redshift-slice. Every galaxy can only be a member of one structure of the catalogue belonging to a given z-slice. Yet it can also belong to other structures in the other z-slices. The third part of the algorithm is the unification of all structures that have at least one member in common. This guarantees that in the final catalogue every galaxy can only belong to one group or cluster.

The underlying idea for the modification of the linking conditions is the following: The a priori redshift slices z_{ini} approximate roughly the mean redshifts $\overline{V}$ of the original FOF-technique. So eq. (1) changes into

$$D_{ij} := 2 \sin \frac{\theta_{ij}}{2} D\left(z_{ini}\right) \leq D_L. \tag{5}$$

$D\left(z_{ini}\right)$ is the distance to z_{ini} in Mpc, being either

$$D\left(z_{ini}\right) := \frac{c z_{ini}}{H_0} \tag{6}$$

in the case of a low-redshift approximation, or more correctly

$$D\left(z_{ini}\right) := d_A\left(H_0, \Omega_M, \Omega_\Lambda, z_{ini}\right) \tag{7}$$

in the case of a cosmologically exact distance measurement. $d_A\left(H_0, \Omega_M, \Omega_\Lambda, z_{ini}\right)$ is the angular distance to z_{ini} for a cosmology with given H_0, Ω_M and Ω_Λ (Carrol et al. 1992). Eq. (3) translates into two equations, one for each of the galaxies i and j:

$$V_i := \left|v_i - c z_{ini}\right| \leq \frac{V_L}{2}, \tag{8}$$

$$V_j := \left|v_j - c z_{ini}\right| \leq \frac{V_L}{2}. \tag{9}$$

If the individual redshift errors δz_i and δz_j of the galaxies i and j are taken into account, the left side of relations (8) and (9) changes:

$$V_i \leq \left[\left(V_L/2\right)^2 + \left(c\delta z_i\right)^2\right]^{1/2} =: V_{L,i}, \tag{10}$$

$$V_j \leq \left[\left(V_L/2\right)^2 + \left(c\delta z_j\right)^2\right]^{1/2} =: V_{L,j}. \tag{11}$$

Obviously, in the case of very small redshift errors, eqs. (8) and (9) are good approximations for eqs. (10) and (11).

A flow chart for the EXT-FOF algorithm is shown in Fig. 2. First, the minimal redshift $z_{ini} = z_{min}$ is chosen for structure finding. A catalogue of groups, that belong to this z_{ini}-slice, is created as follows: An object i, that has not yet been assigned to any group belonging to this redshift-slice, is chosen from the catalogue. Unlike the original FOF, this galaxy also has to be compatible with the chosen z_{ini}, meaning it has to fulfill eq. (10) (or eq. (8)). Then, friends j of that galaxy are searched for. They also have to be compatible with the chosen z_{ini}, i.e. they have to satisfy eq. (11) (or eq. (9)) and have to be closer to galaxy i than the cut-off distance D_L (eq. (5)). If no friends can be found, object i is moved to a list of isolated galaxies. If friends can be found, a group-candidate $k\left(z_{ini}\right)$ is initiated and the galaxies i and j are added to it. The surroundings of the galaxies j are searched for companions fulfilling eqs. (5) and (11) (or (9)), and the loop is repeated until no further friends can be found. A group-candidate is called a real group, if the number $N_{k(z_{ini})}$ of galaxies belonging to it satisfies the relation

$$N_{k(z_{ini})} \geq N_{min} \tag{12}$$

and the group is then added to the catalogue of structures for the given redshift-slice. If this is not the case, the galaxy i and its friends are moved to the list of isolated objects. The next galaxy from the catalogue is then taken and its surroundings are searched for friends. If all galaxies are assigned either to a group or to the isolated list and no galaxies are left in the input catalogue, the search is continued in the next redshift-slice. For this, z_{ini} is increased by a value Δz_{ini} and the original input catalogue of galaxies is restored. The search for friends is then repeated as described above. Once the value of z_{ini} has reached the limit z_{max}, the search is stopped. So far, this technique yields $\left(z_{max} - z_{min}\right)/\Delta z_{ini}$ individual catalogues of clusters. Since one galaxy can belong to different clusters in different redshift-slices, a unification of these groups is necessary to remove this ambiguity. To do this, a group l of any arbitrary z_{ini}-slice is taken. A, so far empty, unified group m is created. All galaxies of the above mentioned group l are added to the unified group m and group l is removed from the group catalogue. Next, the unification procedure looks for a galaxy in unified group m that also belongs to another, non-unified, group n, irrespective of the redshift-slice that this group belongs to. If no such galaxy can be found, unified group m is complete, and the process is repeated for another group l. If there is a galaxy in m that belongs to a group n, as well, all galaxies of group n are added to the unified group m and n gets removed from the catalogue. This loop is repeated until unified group m is complete and none of its members are contained in any of the non-unified groups any more. The result is a catalogue of disjoint structures.

Like Huchra & Geller's version, this new algorithm is commutative and yields reproducible results, i.e. the sequence of the input galaxies does not play a role.

One of this technique's objectives is to reproduce group catalogues found with the Huchra & Geller FOF in the case of spectroscopic datasets. To do this, the values of z_{ini} have to approximate every possible value of $\overline{V}$ for every galaxy pair. Theoretically, this can be reached by using a continuum of z_{ini}-values, ranging from the minimum $\overline{V}$ of the two galaxies in the dataset that have the lowest redshifts to the maximum $\overline{V}$ of the galaxy pair with highest redshifts. Of course this is not feasible in practice. Instead, a discrete set of z_{ini} values is used with a very small spacing Δz_{ini}. The boundaries z_{min} and z_{max} are simply set to the minimum and maximum redshifts of the galaxies used for structure finding.

There are two basic differences between the two FOF techniques: While the Huchra & Geller technique tests, whether eq. (1) is fulfilled for a galaxy pair at only one redshift, the new algorithm tests, whether eq. (5) is satisfied for said galaxy pair at a multitude of redshifts. Furthermore, with the original algorithm, galaxies that are close to one another in projection can be linked together, even though not all of them are close to one another in redshift. Thus, chains of $N \geq N_{min}$ galaxies can be linked together into groups, that are very elongated in the redshift. In the case of the extended FOF, all $N \geq N_{min}$ galaxies have to be compatible with a given redshift z_{ini} in order to be called a group. This makes the above mentioned outcome of elongated galaxy chains highly unlikely and is the reason why the new algorithm is well-suited for cluster finding in photometric redshift surveys. The next Sections (3, 4, and 5) show all of the possible effects resulting from these discrepancies and prove the validity of the extended friends-of-friends for photometric redshift datasets.

3 APPLICATION TO THE CFA1 REDSHIFT SURVEY

3.1 The galaxy catalogue

The CFA1 redshift survey (Huchra et al. 1983) is a magnitude limited, spectroscopic galaxy survey, containing all the galaxies of the Zwicky (Zwicky et al. 1968; Zwicky & Zwicky 1971) or Nilson (1973) catalogues, that satisfy the following selection criteria:

$$m_{pg} \leq 14.5 \text{ mag}\,, \tag{13}$$

and

$$b \geq 40^\circ,\ \delta \geq 0^\circ, \quad \text{or} \quad b \leq -30^\circ,\ \delta \geq -2\overset{\circ}{.}5. \tag{14}$$

The magnitudes are given in the B(0)-Zwicky system. The original catalogue covers 2401 galaxies.

In this paper, an electronic version of the CFA1 galaxy catalogue, created in May 1997, is used. This new catalogue contains 2396 galaxies with corrected magnitudes and redshifts.

3.2 Creation of the group catalogues

Following the recipe of Geller & Huchra (1983), two group catalogues are created, one by using the original FOF technique, the other by applying the new EXT-FOF algorithm. A summary of the Geller & Huchra (1983) treatment of the galaxy data and choice of the linking parameters is given below:

First, the heliocentric galaxy velocities are corrected for a dipole virgocentric flow

$$V_V = V_{in}\left[\sin\delta_i \sin\delta_V + \cos\delta_i \cos\delta_V \cos\left(\alpha_i - \alpha_V\right)\right], \tag{15}$$

where V_{in} is the infall velocity, which is set to 300 km s^{-1}. α_V and δ_V are the right ascension and declination of the Virgo cluster ($\alpha_V = 12^{\rm h}28\overset{\rm m}{.}7$; $\delta_V = 12^\circ 19\overset{\prime}{.}1$; J1950; Ramella et al. 1997), and α_i, and δ_i are the right ascension and declination of galaxy i. Furthermore, a correction for the solar motion with respect to the local group is made (Ramella et al. 1997):

$$V_G = 300 \text{ km s}^{-1} \sin l_i \cos b_i. \tag{16}$$

l_i and b_i are the galactic longitude and latitude of galaxy i. All galaxies with corrected velocities less than 300 km s^{-1} are given an indicative velocity of 300 km s^{-1}. This is done to avoid the singularity at 0 km s^{-1}.

Only galaxies with velocities less than 12000 km s^{-1} are accepted for the cluster search, while the mean velocity of the groups is limited to less than 8000 km s^{-1}.

A Hubble constant of $H_0 = 100$ km s^{-1} Mpc^{-1} is used, to be in accordance with the approach used by Geller & Huchra (1983).

The linking parameters are chosen to vary with redshift, in order to compensate for the variation in the sampling of the luminosity function, as described in Huchra & Geller (1982), and Geller & Huchra (1983):

$$D_L = D_0 R, \tag{17}$$

and

$$V_L = V_0 R, \tag{18}$$

with

$$R = \left[\int_{-\infty}^{M_{ij}} \Phi\left(M\right) dM \left(\int_{-\infty}^{M_{lim}} \Phi\left(M\right) dM\right)^{-1}\right]^{-1/3}. \tag{19}$$

$\Phi\left(M\right)$ is the Schechter luminosity function with $\alpha = -1.30$, $M^* = -19.40$ mag, and $\Phi^* = 0.0143$ Mpc^{-3}.

$$M_{lim} = m_{lim} - 25 - 5\log\left(V_{fid}/H_0\right), \tag{20}$$

and

$$M_{ij} = m_{lim} - 25 - 5\log\left(\overline{V}/H_0\right), \tag{21}$$

in case of the original FOF technique. For cluster finding with the EXT-FOF algorithm, eq. (21) changes to

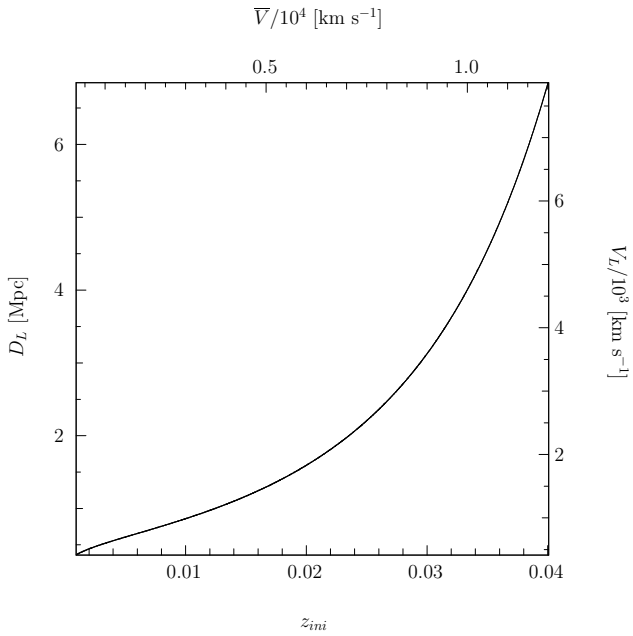

Figure 3. Variation of the linking criteria D_L and V_L for the CFA1 group catalogues, as a function of the FOF mean separation $\overline{V}$, or the EXT-FOF redshift-slicing z_{ini}

$$M_{ij} = m_{lim} - 25 - 5\log\left(cz_{ini}/H_0\right). \tag{22}$$

The fiducial velocity V_{fid} is set to $V_{fid} = 1000$ km s^{-1}, the projected separation D_0 and the velocity difference V_0 at the fiducial velocity are chosen as $D_0 = 0.52$ Mpc and $V_0 = 600$ km s^{-1}. The resulting variation of the linking criteria D_L and V_L as a function of $\overline{V}$, or z_{ini} respectively, is shown in Fig. 3. The described variation of the linking parameters enables the algorithm to detect only structures that have a given minimal number overdensity relative to the mean, completely independent of the structure's redshift.

The CFA1 group catalogue published by Geller & Huchra (1983) contained only groups with more than two members, so we set $N_{min} = 3$.

Since the CFA1 is a local galaxy survey, the low-redshift approximation, eq. (6), is used for the distance calculation in the EXT-FOF. Because of the very small redshift errors of this spectroscopic survey, eqs. (8) and (9) are utilised as the velocity linking criteria. The redshift-spacing is set to $\Delta z_{ini} = 10^{-5}$, to make sure that every possible value of $\overline{V}$ can be approximated.

3.3 Comparison of the group catalogues

The catalogue of structures, resulting from the application of the original FOF algorithm, contains 176 groups and clusters, comprising a total of 1480 galaxies. The composition of these FOF structures is slightly deviant from the ones published by Geller & Huchra (1983). This minor discrepancy is due to the different input galaxy catalogues.

Application of the EXT-FOF algorithm yields 165 groups, containing 1518 galaxies in total. Thus, in the case of the CFA1, the EXT-FOF shows a tendency to identify somewhat larger structures.

In order to compare the algorithms, we do an object-to-object comparison of the group members. We define eight categories for the level of agreement in the group composition:

Table 1. Comparison of the CFA1 FOF and EXT-FOF structures

	category	FOF	EXT-FOF	% FOF	% EXT-FOF
total		176	165	100	100
identical	1	122	122	69.3	73.9
only FOF struct.	2	4	–	2.3	–
only EXT-FOF struct.	3	–	8	–	4.8
FOF struct. larger than EXT-FOF	4	5	5	2.8	3.0
EXT-FOF struct. larger than FOF	5	12	12	6.8	7.3
FOF struct. is combination of EXT-FOF structs.	6	0	0	0.0	0.0
EXT-FOF struct. is combination of FOF structs.	7	28	13	15.9	7.9
FOF and EXT-FOF structs. have some elements in common	8	5	5	2.8	3.0
FOF structs. found with EXT-FOF alg.		172	–	97.7	–

(1) The FOF and EXT-FOF group have identical composition
(2) The group is only found with FOF, i.e. no galaxy in the group is a member of an EXT-FOF group
(3) The group is only found with EXT-FOF, i.e. no galaxy in the group is a member of a FOF group
(4) The EXT-FOF group is a subset of the FOF group, i.e. the FOF group has more members than the EXT-FOF, and none of those surplus members belong to any other EXT-FOF group
(5) The FOF group is a subset of the EXT-FOF group, i.e. the EXT-FOF group has more members than the FOF, and none of those surplus members belong to any other FOF group
(6) The FOF group is a combination of multiple EXT-FOF groups, and can also contain further galaxies that are not part of any other EXT-FOF group
(7) The EXT-FOF group is a combination of multiple FOF groups, and can also contain further galaxies that are not part of any other FOF group
(8) The FOF and EXT-FOF group have some members in common, but do not fall under any of the above mentioned criteria

This classification scheme facilitates the examination of the intrinsic characteristics of the two friends-of-friends algorithms, as can be seen in the next Section 3.4.

Table 1 shows the statistics of the comparison between the FOF and EXT-FOF structures. The first column provides a short description of the categories used. In the second column, the corresponding categories are listed for easy reference. The third and fourth column contain the number of FOF and EXT-FOF groups respectively, that fall under the specified category, while the fifth and sixth column show the percentage of these groups.

122 groups or clusters are recovered identically (category 1) by both algorithms, corresponding roughly to 72% of the FOF or EXT-FOF structures. 17 of the FOF groups are found by the EXT-FOF algorithm either as slightly enlarged (category 5), or reduced (category 4) structures. 28 FOF structures are recovered by the EXT-FOF as a combination of multiple FOF groups (category 7). Further five FOF structures are found by the EXT-FOF, suffering from combinations of the categories 4, 5, 6, and 7 (i.e. category 8). Only four of the 176 FOF groups are not found with the EXT-FOF algorithm (category 2). Thus, a total of 172 FOF structures are recovered by the EXT-FOF algorithm, corresponding to a recovery rate for the EXT-FOF algorithm of almost 98%. On the other hand, the EXT-FOF technique finds eight additional groups (category 3), that are not part of the FOF group catalogue, leading to a spurious detection rate for the EXT-FOF technique of less than 5%, provided that the FOF technique delivers a complete structure catalogue. A closer look at the category 2 groups shows, that they are extremely small. Three of them have only three members and one of them contains four members. Furthermore, they are very elongated in the redshift direction, an attribute that might speak against them as possible galaxy groups, anyway. The category 3 EXT-FOF groups are also very small. Four of them have three members, the other four contain four members. All things considered, in the case of the CFA1 group determination, the EXT-FOF algorithm yields results very similar to the FOF technique. A slight tendency to find larger groups with the EXT-FOF can be seen here. The cause for the discrepancies between the two friends-of-friends techniques is explained in Section 3.4.

3.4 Analysis of the discrepancies

The deviations between the two group catalogues can be ascribed to two effects: Either the EXT-FOF algorithm is able to link two galaxies together, that the original FOF cannot; Or the EXT-FOF algorithm can not link N_{min} (here: $N_{min} = 3$) objects together within one redshift-slice.

If the EXT-FOF algorithm finds a link between two galaxies, yet the FOF does not, then one of the following deviations can result:

(1) The group can only be found with EXT-FOF (i.e. category 3)
(2) The group found with EXT-FOF contains more members than the corresponding FOF group (i.e. category 5)
(3) The EXT-FOF group is a combination of multiple FOF groups (i.e. category 7)

In the first case, the original FOF might find two linked galaxies, but cannot find a third object, that fulfills the linking criteria. Thus the number of objects within the original FOF group-candidate is too small, i.e. eq. (4) is violated, and the group is rejected. If the EXT-FOF method is able to find a third object in the current redshift-slice, that is linked to one of the galaxies in the pair, the number of group members satisfies eq. (12) and the group is accepted. It is also possible, that the original FOF finds two galaxy pairs, but is not capable of connecting them, while the EXT-FOF algorithm is able to link two galaxies of each pair, thus creating a group-candidate containing four galaxies. Eq. (12) is then satisfied and the EXT-FOF group is accepted.

In the second case, the EXT-FOF is able to find one or more galaxies, that are defined as isolated by the FOF algorithm, linked

to group members, resulting in a larger group in the EXT-FOF catalogue.

In the third case, the original FOF finds two or more separate groups. If the EXT-FOF can find links between members of the different FOF groups, those groups are combined into one big EXT-FOF structure. Of course, it is also possible, that further galaxies, defined as isolated by the original FOF, get attached to such a big structure, following the reasoning of the second case. This leads to EXT-FOF groups, that consist of a number of FOF groups and some additional galaxies.

If the EXT-FOF algorithm cannot find N_{min} galaxies linked together within at least one of the redshift-slices, one of the following deviations can result:

(1) The group can only be found with the original FOF (i.e. category 2)
(2) The group found with FOF contains more members than the corresponding EXT-FOF group (i.e. category 4)
(3) The FOF group is a combination of multiple EXT-FOF groups (i.e. category 6)

In the first case, the original FOF finds at least $N_{min} = 3$ objects that are linked together, satisfying eq. (4). The EXT-FOF, on the other hand, can only find pairs of galaxies in various redshift slices. Since every group-candidate has to fulfill eq. (12) in at least one redshift slice, these galaxy pairs are not taken into account in the unification process, and these galaxies are defined as isolated by the EXT-FOF algorithm.

In the second case, one galaxy, defined as group member by the FOF, cannot be attached to an EXT-FOF group. This is due to the fact, that there is no redshift slice, where this galaxy can be linked to at least two (in general: $N_{min} - 1$) members of this EXT-FOF structure. Thus the object is not entered into the pre-unification catalogue and is not included in the EXT-FOF group. It is also possible, that more than one galaxy of the FOF group is missing in the corresponding EXT-FOF group. This can happen, if the above mentioned situation is true for all of those galaxies and, additionally, there is no redshift slice where two or more of those missing galaxies are linked with one of the EXT-FOF group members. However, in the case of the CFA1 group catalogues, none of the five FOF groups, that fall under category 4, are larger than their EXT-FOF counterpart by more than one group member.

In the third case, the EXT-FOF finds two or more separate groups, while the FOF is able to link them together into one structure. This can happen, if there are no redshift slices, where at least two members of one EXT-FOF group can be linked with at least one member of another group. Following the reasoning of the second case, it is furthermore possible, that the large FOF group can contain additional members, that are defined as isolated by the EXT-FOF. As far as the CFA1 catalogues are concerned, this effect never shows up, though.

Category 8 groups are generated by a combination of the two effects: Members get lost in the EXT-FOF groups, because of too few linked objects at a given redshift slice, and at the same time new links can be found to galaxies, that are defined as isolated by the original FOF, while some subset of the FOF and EXT-FOF group is identical.

In one of the cases examined for category 3 of the CFA1 comparison, a group found with the original FOF, is removed from the group list because its mean velocity exceeds the limit. The EXT-FOF is able to find another galaxy linked to this group, pushing the group mean velocity below the limit. Thus, the group is included in the EXT-FOF, yet not in the FOF group catalogue. However, this is a border effect and could in principle also work in the other direction, removing groups from the EXT-FOF catalogue (i.e. category 2).

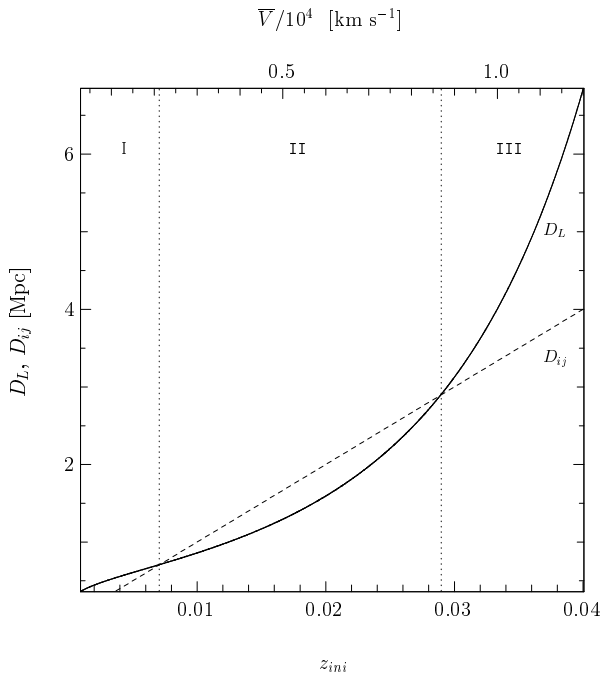

Figure 4. Comparison of the CFA1 projected linking distance D_L (solid line) and the projected separation D_{ij} (dashed line) of the galaxies i and j, as a function of the the mean distance $\overline{V}$, or the redshift slice z_{ini}, respectively. The angular separation θ_{ij} of the chosen galaxy pair leads to two intersections between D_L and D_{ij}, dividing the graph into three areas (dotted lines). The projected linking criterion $D_{ij} \leq D_L$ is satisfied in the areas I and III. It is not satisfied in area II.

The reason, why the EXT-FOF algorithm is sometimes able to find links between objects, while the original FOF is not, can be explained as follows:

The equations used here for the calculation of the projected distance D_{ij}, eqs. (1), (5), and (6), show that $D_{ij} \propto \overline{V}$ and $D_{ij} \propto z_{ini}$, respectively. However, being varied with the luminosity function, the linking distance D_L is not proportional to the redshift. D_L is growing monotonically with z, switching from a convex curvature at low redshifts, to concave at higher redshifts. The slope of D_{ij} is set by the angular separation θ_{ij} of the two galaxies. There are three possible scenarios for the behaviour of D_{ij} and D_L:

Either θ_{ij} is so small, that $D_{ij} \leq D_L$ over the entire redshift range of $\overline{V} \in \left[300 \text{ km s}^{-1}, 12000 \text{ km s}^{-1}\right]$, or $z_{ini} \in [0.001, 0.04]$ respectively, i.e. the projected linking criterion, eq. (1) or (5), is fulfilled at $\overline{V}$ and in all other redshift slices z_{ini}.

Or θ_{ij} is so large, that $D_{ij} > D_L$ over the entire redshift range. This galaxy pair can neither be linked together by the FOF, nor by the EXT-FOF algorithm.

Or θ_{ij} lies between the above mentioned values. In this case, D_{ij} intersects D_L twice.

The third scenario can lead to the links, that can only be found with the EXT-FOF algorithm. In this case, the redshift range can be divided into three areas, which is shown in Fig. 4. The figure shows a comparison of the projected linking distance D_L (solid line) and the projected separation D_{ij} (dashed line) of the galaxies i and j,

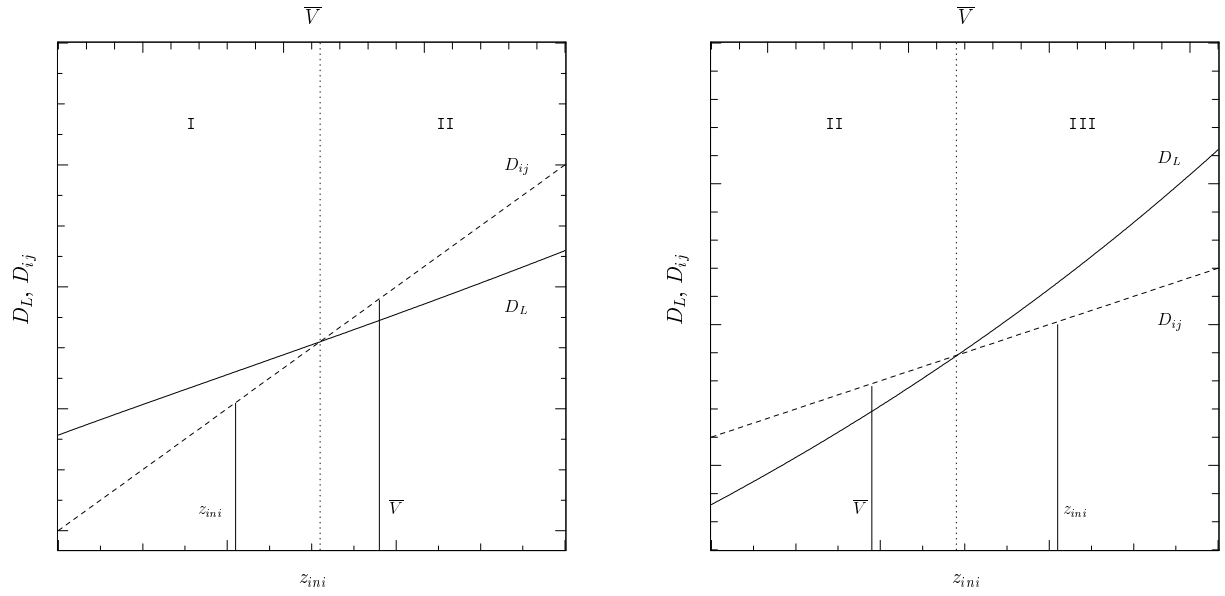

Figure 5. Comparison of the CFA1 projected linking distance D_L (solid line) and projected separation D_{ij} (dashed line), as a function of the the mean distance $\overline{V}$, or the redshift slice z_{ini}, for two example galaxy pairs. These schematic drawings show magnified excerpts of the transition regions (dotted lines) between the areas I and II (left panel), and the areas II and III (right panel), that are described in Fig. 4. **Left panel:** The projected separation D_{ij} at the mean redshift $\overline{V}$ (denoted by the solid vertical line in area II) of the galaxies i and j, does not fulfill the projected linking criterion $D_{ij} \leq D_L$. Thus, the original FOF cannot link the two galaxies. In the case shown here, the range of z_{ini} values, satisfying the EXT-FOF redshift-space linking criteria, eqs. (8) and (9), reaches into area I. For simplification, only one of those redshift slices z_{ini} and the corresponding value of D_{ij} is shown here (solid vertical line in area I). $D_{ij} \leq D_L$ is fulfilled for this redshift, and the galaxies i and j are found as linked by the EXT-FOF algorithm. **Right panel:** $\overline{V}$ is again lying in area II, thus the original FOF cannot link this galaxy pair. The range of z_{ini} values, that satisfy the EXT-FOF redshift-space linking criteria, reach into area III in this case. Once more, only one of those redshift slices z_{ini} and the corresponding value of D_{ij} is shown here (solid vertical line in area III). $D_{ij} \leq D_L$ is fulfilled for this redshift, and the galaxy pair i and j are found as linked by the EXT-FOF algorithm.

as a function of the the mean distance $\overline{V}$, or the redshift slice z_{ini}, respectively. In the areas I and III, the projected linking criterion $D_{ij} \leq D_L$ is fulfilled. Whereas in area II it is never fulfilled. It becomes obvious, that it is critical in which of those areas the linking criteria are tested. The original FOF can only test the projected linking criterion at a fixed redshift $\overline{V}$, set by the galaxy pair. The EXT-FOF, on the other hand, tests the linking criteria at all redshifts. If the EXT-FOF redshift-space linking criteria, eqs. (8) and (9), can be fulfilled for a given galaxy pair, then they are generally satisfied for an interval of z_{ini} values. If eq. (5) can also be satisfied for at least one of those redshifts z_{ini}, then all criteria are fulfilled and the galaxy pair is found as linked by the EXT-FOF. Thus, only the EXT-FOF and not the original FOF is able to link a galaxy pair in one of the two following situations: The mean velocity $\overline{V}$ is lying in the area II, and the redshift interval of z_{ini} values, that satisfy eqs. (8) and (9), reaches either into area I (Fig. 5, left panel), or into area III (Fig. 5, right panel). As a result, the projected linking criterion is not satisfied for the original FOF, while both linking criteria can be fulfilled in at least one z_{ini} slice, in the case of the EXT-FOF.

It can be easily seen, that this effect does not exist, if D_L and D_{ij} follow the same variation with redshift, $D_L(z) \propto D_{ij}(z)$.

In the following, we explain why the EXT-FOF algorithm sometimes can not link together $N_{min} = 3$ objects within at least one z_{ini} slice, and why this is the reason for some of the above mentioned deviations from the original FOF.

The original FOF algorithm can move relatively freely along the redshift axis, when looking for friends. For example, we consider a set of galaxies a, b, and c, with given velocities v_a, v_b, and v_c. For matters of simplicity, we assume $v_a < v_b < v_c$. The FOF calls those three galaxies a group, if there is at least one galaxy among them, that can be linked to the other two. If, for example, the galaxies a and b, and b and c fulfill the linking criteria, i.e. eqs. (1) and (3), then a, b and c are linked together. It is not necessary, that a and c also satisfy the linking criteria, and $V_{ac} > V_L$ is possible. Thus, in principle, the FOF allows for very elongated chains of galaxies along the redshift axis, as long as these galaxies have a small projected separation and the velocity difference V_{ij} between next neighbours satisfies eq. (3). This effect is what makes the original FOF unqualified for cluster finding in datasets with rather uncertain redshifts, like photometric galaxy catalogues.

The EXT-FOF algorithm cannot move so freely along the redshift axis. By only looking for friends among galaxies, that are compatible with a given redshift slice, the probability of finding very elongated structures is efficiently reduced.

To illustrate the problem, Fig. 6 shows the case of a set of galaxies, a, b, and c, that are found as a group by the FOF, yet not by the EXT-FOF. For simplification, we choose a galaxy set, that has a very small spread in the projected distance, so that eqs. (1) and (5) are fulfilled for all three galaxies, and we only have to test, whether the velocity linking criteria are fulfilled. The figure shows the variation of the linking velocity V_L (solid line) with redshift z_{ini}, or mean velocity $\overline{V}$, respectively. The individual velocities v_a, v_b, and v_c of the three galaxies are shown on the lower scale. The filled squares are the original FOF velocity separations V_{ab}, V_{bc}, and V_{ac}, resulting from eq. (3), and plotted at the corresponding mean velocities. It becomes obvious, that V_{ab} and V_{bc} satisfy the velocity linking criterion, and together with the already

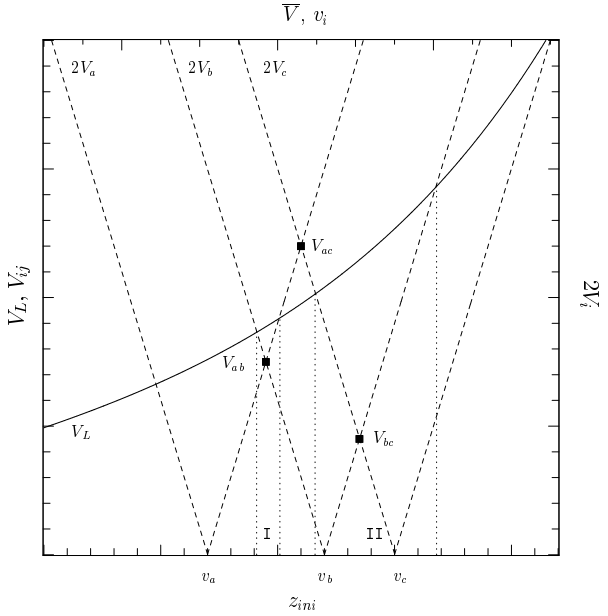

Figure 6. Comparison of the CFA1 linking velocity V_L (solid line) with the original FOF (filled squares) and EXT-FOF (dashed lines) velocity separations, V_{ij} and V_i, for a set of three galaxies, a, b, and c, that can only be linked with the original FOF, yet not with the EXT-FOF. The lower scale shows the redshift z_{ini}, the upper scale shows the corresponding mean velocity $\overline{V}$. The individual velocities v_a, v_b, and v_c of the three galaxies are also shown on the lower scale. The original FOF velocity separations V_{ab}, V_{bc}, and V_{ac}, resulting from eq. (3), are plotted at the corresponding mean velocities. The EXT-FOF velocity separations are plotted as $2\,V_a$, $2\,V_b$, and $2\,V_c$ to make an easy comparison with V_L possible. The dotted lines show the areas, where eqs. (8) and (9) are satisfied for two galaxies: In area I, the requirement is fulfilled for the galaxies a and b, and in area II it is fulfilled for the galaxies b and c. In no redshift slice, can all $N_{min} = 3$ galaxies satisfy the EXT-FOF velocity linking requirement $V_i \leq V_L/2$.

fulfilled projected linking criterion, the original FOF combines the three galaxies into a group. The dashed lines denote the EXT-FOF velocity separations. They are plotted as $2\,V_a$, $2\,V_b$, and $2\,V_c$ to make an easy comparison with V_L possible. The dotted lines show the areas where eqs. (8) and (9) are satisfied for two galaxies: In area I, the requirement is fulfilled for the galaxies a and b, and in area II it is fulfilled for the galaxies b and c. There is no redshift slice, where all three galaxies satisfy the EXT-FOF velocity linking requirement $V_i \leq V_L/2$. As a result, the EXT-FOF can only find the galaxies a and b, or b and c linked together, in the z_{ini} ranges given by the areas I, or II. Those galaxy pairs do not satisfy eq. (12) with $N_{min} = 3$, and thus are not added to the group list.

Theoretically, another effect, that could remove a single link between two galaxies, is conceivable. It would also lead to the observed phenomena of category 2, 4, 6, or 8. If the step size Δz_{ini} of the EXT-FOF redshift slicing is chosen too large, not every possible value of $\overline{V}$ can be approximated anymore, and a link found with the original FOF could not be recovered with the EXT-FOF algorithm. This is never the case in one of the examined catalogues, though, proving that the chosen step size is sufficiently small and does not lead to unwanted numerical effects.

4 APPLICATION TO THE LCRS REDSHIFT SURVEY

4.1 The galaxy catalogue

The LCRS (Shectman et al. 1996) is an R-band selected, spectroscopic galaxy survey. It consists of six $1\overset{\circ}{.}5 \times 80^\circ$ strips, three of which are lying in the north, the other three in the south Galactic cap. The survey covers a total area of over $700\,\mathrm{deg}^2$, divided into 327 individual fields. For 120 of those fields spectroscopy is done with a 50 fibre multiobject spectrograph (MOS), and they have nominal apparent magnitude limits of

$$16.0 \text{ mag} \leq m_R \leq 17.3 \text{ mag}. \tag{23}$$

For the remaining 207 fields spectroscopy is done with a 112 fibre MOS, with nominal apparent magnitude limits of

$$15.0 \text{ mag} \leq m_R \leq 17.7 \text{ mag}. \tag{24}$$

For every setup, all of the fibres are used, but since each of the fields is observed only once, there is a field-to-field variation in the selection criteria. The protective tubing around the individual fibres of the MOS makes it impossible to observe spectra of objects, that are closer to each other than $55''$, leading to $55''$ "orphans", that have no spectroscopic redshifts. The surveyed galaxies are sampled randomly within each field.

The catalogue we use here is a combination of the 23695 galaxies that have spectroscopic redshifts and the 1694 $55''$ "orphans", resulting in a total of 25389 galaxies. Both datasets only include objects, that are lying within the geometric and photometric boundaries of the survey. Artificial redshifts are assigned to the $55''$ "orphans", by giving each of them the redshift of its nearest neighbour, convolved with a Gaussian of width $\sigma = 200$ km s^{-1} (Tucker et al. 2000, Tucker, priv. comm.).

4.2 Creation of the group catalogues

Following the recipe of Tucker et al. (2000), we once more create two structure catalogues, one with the original FOF algorithm, the other with our EXT-FOF. In the following, an overview of the Tucker et al. (2000) treatment of the data is shown. Furthermore, the application of this recipe to the EXT-FOF is explained.

First, all galaxy velocities are corrected for motion relative to the dipole moment of the cosmic microwave background. The equation used by Tucker et al. (2000) is given in galactic coordinates

$$V_V = V_\odot \left[\sin b_i \sin b_\odot + \cos b_i \cos b_\odot \cos\left(l_i - l_\odot\right)\right], \tag{25}$$

where $V_\odot = 368.9$ km s^{-1}, $b_\odot = 48\overset{\circ}{.}05$, and $l_\odot = 264\overset{\circ}{.}33$ (Lineweaver et al. 1996, Tucker, priv. comm.), and b_i, l_i are the galactic latitude and longitude of galaxy i.

The set of galaxies used for cluster finding is limited to objects having corrected velocities v_i such that

$$7500 \text{ km s}^{-1} \leq v_i < 50000 \text{ km s}^{-1}, \tag{26}$$

and absolute magnitudes M_i between

$$-22.5 \text{ mag} + 5\log h \leq M_i < -17.5 \text{ mag} + 5\log h. \tag{27}$$

Not taking any colour corrections into account, we simply set

$$M_i = m_i - 5\log\left(d_L\left(H_0, \Omega_M, \Omega_\Lambda, v_i/c\right)\right) + 5, \tag{28}$$

where m_i is the apparent magnitude of galaxy i, and $d_L\left(H_0, \Omega_M, \Omega_\Lambda, v_i/c\right)$ is the luminosity distance for the given

cosmology to galaxy i (Carrol et al. 1992). Since the LCRS is relatively deep, going out to redshifts of roughly 0.2, it becomes necessary to use cosmologically correct expressions.

Only groups with mean velocities $\overline{V_g}$ such that

$$10000 \text{ km s}^{-1} \leq \overline{V_g} < 45000 \text{ km s}^{-1} \tag{29}$$

are accepted in the final group catalogue.

We use a flat cosmology with $H_0 = 65 \text{ km s}^{-1} \text{ Mpc}^{-1}$, $\Omega_M = 0.3$, and $\Omega_\Lambda = 0.7$.

The distance equations for the original FOF have to be modified to take the cosmologically correct expressions into account. Eq. (1) becomes

$$D_{ij} = 2 \sin \frac{\theta_{ij}}{2} D_{ave} \leq D_L, \tag{30}$$

with the mean comoving angular distance D_{ave} between the galaxies i and j

$$D_{ave} := \frac{d_A\left(H_0, \Omega_M, \Omega_\Lambda, \frac{v_i}{c}\right) + d_A\left(H_0, \Omega_M, \Omega_\Lambda, \frac{v_j}{c}\right)}{2} \tag{31}$$

replacing the $\overline{V}$ of eq. (2).

In the case of the EXT-FOF, we use $D\left(z_{ini}\right)$ of eq. (7) for the calculation of the projected distance D_{ij}. The individual spectroscopic redshift errors of the galaxies are not yet taken into account, thus eqs. (8) and (9) still apply. A stepsize of $\Delta z_{ini} = 10^{-5}$ is used.

The linking parameters are varied with redshift. Yet, due to the field-to-field variations in the sampling fraction, the photometric limits, and the number of MOS fibres, this dependency is more complicated than in the case of the CFA1. Eqs. (17) and (18) are used for the variation of D_L and V_L, and R is given by

$$R = \left[\frac{n^{exp}\left(f, D\right)}{n^{exp}_{fid}}\right]^{-1/3}. \tag{32}$$

$n^{exp}\left(f, D\right)$ is the expected galaxy number density in the field f at a comoving distance D. D is either D_{ave} in the case of the original FOF, or $D\left(z_{ini}\right)$ in the case of the EXT-FOF. n^{exp}_{fid} is the galaxy number density $n^{exp}\left(f, D\right)$ in a fiducial field at a given fiducial distance. $n^{exp}\left(f, D\right)$ is calculated with the help of the Schechter luminosity function $\Phi\left(M\right)$:

$$n^{exp}\left(f, D\right) = F \int_{M_{min}}^{M_{max}} \Phi\left(M\right) dM, \tag{33}$$

where F is the sampling fraction of field f. M_{min} and M_{max} are the absolute photometric limits of this field, at the given comoving distance D. When comparing two galaxies from two different fields f_a, and f_b, the average of the expected galaxy densities is taken:

$$n^{exp}\left(f, D\right) = \frac{n^{exp}\left(f_a, D\right) + n^{exp}\left(f_b, D\right)}{2}. \tag{34}$$

Two Schechter luminosity functions are used (Lin et al. 1996; Tucker et al. 1997), following the approach of Tucker et al. (1997). One is valid for the 50 fibre fields in the southern Galactic cap, and has $\alpha = -0.74$, $M^* = -20.55 \text{ mag} + 5 \log h$, and $\Phi^* = 0.016\, h^3 \text{Mpc}^{-3}$. The other is used for the 50 fibre fields in the northern Galactic cap, as well as for all 112 fibre fields. Its parameters are $\alpha = -0.70$, $M^* = -20.29 \text{ mag} + 5 \log h$, and $\Phi^* = 0.019\, h^3 \text{Mpc}^{-3}$.

For the fiducial field the latter luminosity function is used. Furthermore, this field has a sampling fraction of $F = 1$, and apparent magnitude limits of

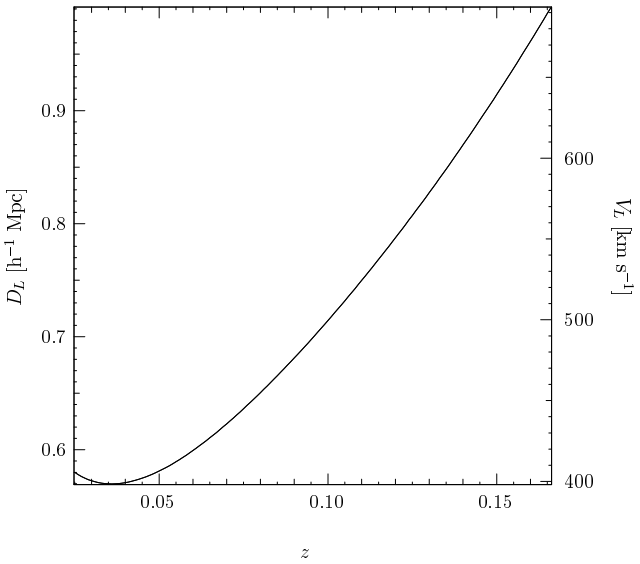

Figure 7. Variation of the linking criteria D_L and V_L for the LCRS group catalogues, as a function of redshift z. As a reminder, in this case R is not only a function of distance, but also depends on the field. We show a typical example field, having a MOS setup with 112 fibres, a sampling fraction of $F = 0.7$, and photometric limits of $m_{min} = 15.0$ mag, $m_{max} = 17.7$ mag.

$$15.0 \text{ mag} \leq m_R \leq 17.7 \text{ mag}. \tag{35}$$

The fiducial redshift is set to $c\, z_{fid} = 30000 \text{ km s}^{-1}$.

Only groups having at least $N_{min} = 3$ members are searched for. The projected separation D_0 and the velocity difference V_0 are chosen as $D_0 = 0.715 h^{-1}$Mpc and $V_0 = 500 \text{ km s}^{-1}$, respectively, again following Tucker et al. (1997).

The resulting variation of the linking criteria D_L and V_L as a function of redshift z is shown in Fig. 7. This graphic is created for an example field having a MOS setup with 112 fibres and photometric limits $m_{min} = 15.0$ mag, $m_{max} = 17.7$ mag. We use a typical sampling fraction of $F = 0.7$.

4.3 Comparison of the group catalogues

Application of the original FOF yields a total of 1367 groups. 6747 galaxies are contained in these groups. The structures are slightly deviant from the ones published by Tucker et al. (2000). These discrepancies in the group composition arise from three differences in the treatment of the data: First, we include no colour corrections in eq. (28), unlike Tucker et al. (2000). Second, for the determination of D_{ave} and $D\left(z_{ini}\right)$ we make use of the comoving angular distance $d_A\left(H_0, \Omega_M, \Omega_\Lambda, z\right)$, while Tucker et al. (2000) utilised the proper motion distance $d_M\left(H_0, \Omega_M, \Omega_\Lambda, z\right)$. Third, we determine group memberships in a flat universe with a low matter content, whereas Tucker et al. (2000) used an Einstein-de Sitter universe.

The catalogue resulting from the EXT-FOF application contains 1285 groups, with a total of 6337 galaxies.

Table 2 shows the statistics of the comparison between the FOF and EXT-FOF structures in the case of the LCRS. The same object-to-object comparison is used as described in Section (3.3).

1280 of the FOF groups are recovered with the EXT-FOF algorithm, corresponding to a recovery rate of almost 94%. The EXT-FOF, on the other hand, finds only one group, that is not a member of the FOF group catalogue (category 3), leading to a spurious de-

Table 2. Comparison of the LCRS FOF and EXT-FOF structures

	category	FOF	EXT-FOF	% FOF	% EXT-FOF
total		1367	1285	100	100
identical	1	1145	1145	83.8	89.1
only FOF struct.	2	87	–	6.4	–
only EXT-FOF struct.	3	–	1	–	0.1
FOF struct. larger than EXT-FOF	4	120	120	8.8	9.3
EXT-FOF struct. larger than FOF	5	4	4	0.3	0.3
FOF struct. is combination of EXT-FOF structs.	6	5	10	0.4	0.8
EXT-FOF struct. is combination of FOF structs.	7	2	1	0.2	0.1
FOF and EXT-FOF structs. have some elements in common	8	4	4	0.3	0.3
FOF structs. found with EXT-FOF alg.		1280	–	93.6	–

tection rate of less than 1%. Both the recovery and spurious detection rates are based on the assumption that the original FOF algorithm used here yields a complete structure catalogue. 1145 structures are found identical by both algorithms, so the rate of identical recoveries lies at roughly 86%. Of the 87 FOF groups, that have no EXT-FOF counterparts (category 2), 77 have only three members, and the remaining ten contain four objects each. Those groups are all very elongated in redshift, making their group status questionable, anyway. The one group falling under category 3 is also extremely small, having only three members. The above comparison shows, that both algorithms yield very similar results.

4.4 Analysis of the discrepancies

Like in the case of the CFA1, all of the deviations mentioned above can be explained by the two effects, that are described in Section 3.4.

The reason for finding an additional link with the EXT-FOF in the LCRS catalogue is very similar to the case of the CFA1. The equations used for the determination of the projected distance D_{ij}, eqs. (30), (31), and (5), (7), show that D_{ij} grows with $d_A\,(H_0, \Omega_M, \Omega_\Lambda, z)$, while the linking distance D_L is varied with the luminosity function. D_{ij} has a convex curvature, D_L is concave. The slope of D_{ij} is once more set by the angular separation θ_{ij}, and there are again three possible scenarios for the behaviour of D_{ij} and D_L. Very small angular separations lead to $D_{ij} \leq D_L$, and very large values of θ_{ij} lead to $D_{ij} > D_L$ for the entire redshift range, that is used for cluster finding. Fig. 8 shows the case of an example galaxy pair with a medium sized angular separation, leading to one intersection between D_{ij} (dashed line) and D_L (solid line). The intersection divides the graph into two areas (dotted line). In area I the projected linking criterion $D_{ij} \leq D_L$ is satisfied, in area II it is not. Thus, whenever the original FOF is limited to comparing D_{ij} with D_L at a value of D_{ave}, that corresponds to a redshift in area II, and the redshift-space linking criteria, eqs. (8) and (9), allow the EXT-FOF to compare D_{ij} with D_L in area I, only the EXT-FOF can find a link between the galaxies i and j.

The explanation, why the EXT-FOF cannot link together certain objects in the LCRS catalogue, while the original FOF can, is completely analogous to the case of the CFA1: The original FOF can move relatively freely through redshift space in order to link galaxies to one another. The EXT-FOF, on the other hand, is always limited to fulfilling both linking criteria for at least N_{min} objects within one redshift slice.

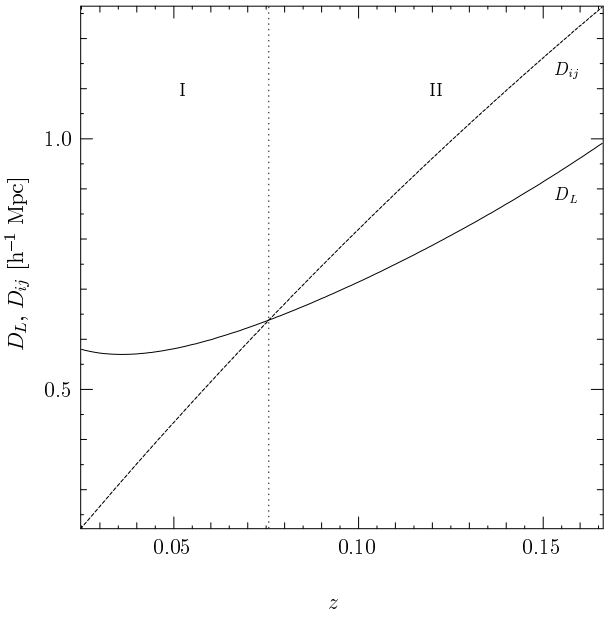

Figure 8. Comparison of the LCRS projected linking distance D_L (solid line) and the projected separation D_{ij} (dashed line) of the galaxies i and j, as a function of the redshift z. The angular separation θ_{ij} of the chosen galaxy pair leads to one intersection between D_L and D_{ij}, dividing the graph into two areas (dotted line). The projected linking criterion $D_{ij} \leq D_L$ is satisfied in area I, yet not in area II. This example galaxy pair is lying in a field, with a MOS setup of 112 fibres, a sampling fraction of $F = 0.7$, and photometric limits of $m_{min} = 15.0$ mag, $m_{max} = 17.7$ mag.

5 LCRS WITH SIMULATED PHOTOMETRIC REDSHIFTS

In order to prove the validity of the EXT-FOF algorithm for structure finding in photometric redshift datasets, we create artificial photometric redshifts for all galaxies contained in our LCRS galaxy catalogue. We determine a group catalogue, based on this new dataset, with the help of the EXT-FOF algorithm, taking into account the photometric redshifts and their errors. A comparison between this structure catalogue and the EXT-FOF catalogue described in Section 4.2 shows the applicability of the EXT-FOF technique in case of galaxy catalogues with photometric redshifts.

5.1 Creation of the galaxy dataset with simulated photometric redshifts

For every LCRS galaxy a random redshift offset is created. The offsets follow a Gaussian distribution with a σ of roughly 5% of the survey depth. That percentage resembles the typical proportions between the redshift errors and the depth of a photometric redshift survey. In the case of the LCRS, the width of the Gaussian is set to $c\sigma = 2500$ km s^{-1}. The photometric redshifts are then created by adding the individual offsets to the spectroscopic redshifts of the galaxies. Furthermore, the redshift errors δz_i are all set to σ. Except for the redshifts of the galaxies and their errors, the galaxy dataset remains unchanged.

5.2 Creation of the group catalogue

To construct the EXT-FOF structure catalogue of this pseudo-photometric redshift dataset, we follow the recipe described in Section 4.2.

The new galaxy dataset is given the same treatment as the spectroscopic one, as far as the velocity correction, and the culling of galaxies on the basis of the velocity and absolute magnitude limits is concerned. Due to this selection process, the subset of galaxies that enters the structure finding procedure can be deviant from the one used in the spectroscopic redshift case. A total of 22739 galaxies are used for cluster finding in the spectroscopic redshift case, 22617 galaxies are used in the photometric redshift case. 20255 galaxies are common to both culled datasets.

For the calculation of the projected distance D_{ij}, we use $D\left(z_{ini}\right)$ of eq. (7). The relatively large redshift errors are taken into account, and relations (10) and (11) apply for the linking velocities $V_{L,i}$ and $V_{L,j}$. The stepsize Δz_{ini} is again set to 10^{-5}.

The same low matter density cosmology is used as described in Section 4.2. We furthermore use the same linking parameters and group mean velocity limits. The minimum number of objects is once more set to $N_{min} = 3$.

5.3 Comparison of the group catalogues

Section 4.3 shows that in case of the spectroscopic dataset the EXT-FOF algorithm yields a group catalogue, that is very similar to the FOF group catalogue. Thus, in principle, the groups resulting from the photometric redshift dataset could be compared to either the FOF, or the EXT-FOF group catalogue of the spectroscopic dataset. For the following examination we choose the latter.

The EXT-FOF algorithm finds a total of 1598 structures in the simulated photometric redshift galaxy catalogue. The groups and clusters contain 10831 galaxies. This corresponds to a mean of almost seven objects per structure. In the spectroscopic redshift case, structures contain a mean of almost five objects. Obviously, the EXT-FOF algorithm tends to find more and larger structures in photometric redshift datasets.

The comparison between the EXT-FOF structures resulting from the spectroscopic redshift dataset and the structures resulting from the photometric one is shown in table 3. Again, we use the "category 1 - 8" classification scheme, that we already described in Sect. 3.3, replacing "FOF" with "EXT-FOF with spectroscopic redshift dataset" and "EXT-FOF" with "EXT-FOF with photometric redshift dataset".

Only 94 of the 1285 EXT-FOF structures with spectroscopic redshifts cannot be retrieved (category 2), leading to a recovery rate of almost 93%. 646 additional groups are found in the photometric galaxy dataset (category 3), corresponding to a spurious detection rate of 40%. The recovery and spurious detection rates are based on the assumption that the application of the EXT-FOF algorithm to the spectroscopic dataset results in a complete structure catalogue. The similarity between the original FOF groups and the EXT-FOF groups in the case of the spectroscopic galaxy dataset was already confirmed in Sect. 4.3. The number of structures, that are identical in both group catalogues is roughly 16%. Due to the strongly differing input galaxy catalogues, this small percentage does not come as a surprise. Both the category 2 and 3 structures tend to be relatively small. 96.8% of the category 2 and 81.6% of the category 3 groups have less than five members.

Under the assumption that the structures found by the FOF and EXT-FOF algorithms in the spectroscopic galaxy dataset are real, this comparison shows that the EXT-FOF algorithm is capable of finding almost all of the structures contained in this photometric redshift dataset. Roughly 60% of the found structures can be expected to be real. This demonstrates that the EXT-FOF technique is a very conservative cluster finder and can be used for identification of cluster candidates in photometric redshift galaxy datasets.

5.4 Analysis of the discrepancies

Some of the discrepancies in the two group catalogues are due to the slightly different composition of the culled input galaxy datasets. After all, the composition of those datasets differs by roughly 10%. However, since this is only a border effect, we do not wish to give it further attention here.

The really interesting discrepancies can be ascribed to either one, or both, of the following two reasons:

One is the scattering of the newly created photometric redshifts against the real, spectroscopic ones.

The other is the fact that the redshift errors are finally taken into account when testing the velocity linking criteria, using relations (10) and (11).

Due to the Gaussian nature of the simulated photometric redshift distribution, almost 32% of the galaxies have new redshifts, that deviate by more than 1σ from their original spectroscopic ones. However, eqs. (10) and (11) only allow for a deviation from z_{ini} of roughly 1σ ($V_L/2$ is relatively small compared to $c\delta z_i = c\delta z_j = c\sigma$). So there is a non-negligible amount of galaxies in the photometric redshift dataset, that are found as linked in the spectroscopic redshift cluster catalogue, yet cannot be linked together anymore, because of their large scatter in photometric redshift. On the other hand, this scatter can also link galaxies together, that are defined as separated in the spectroscopic redshift dataset. So the scattering is responsible for both, finding and losing links between galaxies, and can result in any type of deviation ranging from category 2 to 8.

Taking the redshift errors into account leads to much larger velocity linking criteria $V_{L,i}$ and $V_{L,j}$, than in the spectroscopic redshift case where we use $V_L/2$ as linking criterion. Thus, the new velocity linking criteria are by far less strict, and the probability of finding two objects as linked is increased. The new velocity linking criteria are responsible for finding additional links and result in deviations of category 3, 5, and 7. In combination with the above mentioned scattering of photometric redshifts they can also result in category 8 discrepancies. The consideration of the photometric redshift errors is the main reason for the obviously larger and more numerous structures found in the photometric redshift structure catalogue.

Table 3. Comparison of the LCRS EXT-FOF structure catalogues with and without simulated photometric redshifts

	category	EXT-FOF without δz	EXT-FOF with δz	% EXT-FOF without δz	% EXT-FOF with δz
total		1285	1598	100	100
identical	1	230	230	17.9	14.4
only EXT-FOF without δz struct.	2	94	–	7.3	–
only EXT-FOF with δz struct.	3	–	646	–	40.4
EXT-FOF without δz struct. larger than EXT-FOF with δz	4	34	34	2.7	2.1
EXT-FOF with δz struct. larger than EXT-FOF without δz	5	382	382	29.7	23.9
EXT-FOF without δz struct. is combination of EXT-FOF with δz structs.	6	0	0	0.0	0.0
EXT-FOF with δz struct. is combination of EXT-FOF without δz structs.	7	229	92	17.8	5.8
EXT-FOF with and without δz structs. have some elements in common	8	316	214	24.6	13.4
EXT-FOF without δz structs. found with EXT-FOF with δz alg.		1191	–	92.7	–

6 SUMMARY

In this paper we presented a new structure finding algorithm designed to detect groups and clusters of galaxies in a galaxy catalogue having photometric redshifts.

Since the development of the photometric redshift technique this type of galaxy survey has grown in popularity. The relatively large errors in the redshift evaluation pose a problem for a reliable cluster identification, though. One of the most common cluster finding methods is the friends-of-friends (or FOF) technique. It utilises a straightforward approach by looking for overdensities in the galaxy distribution and not depending on any model assumptions for clusters, and it proved to yield reliable results. However this algorithm is only capable of looking for structures in either spectroscopic redshift datasets, or simulated galaxy datasets. We thus created a modified algorithm, the extended friends-of-friends (or EXT-FOF), based on the original FOF, that is a tailor-made solution for dealing with the large photometric redshift errors.

We presented our new algorithm and explained the major differences between the original FOF and the EXT-FOF method. The basic working principle of the EXT-FOF being the limitation to galaxies for structure finding, that are compatible within their redshift errors with given redshift values.

The EXT-FOF algorithm was tested on two spectroscopic redshift surveys, the Center for Astrophysics Redshift Survey (CFA1) and the Las Campanas Redshift Survey (LCRS). The resulting groups were compared to structures found with the original FOF in those two surveys. We were able to show that in case of spectroscopic redshift datasets, the FOF and EXT-FOF group catalogues were almost identical to each other. The comparison provided a recovery rate of almost 98% and 94% of the FOF structures for the CFA1 and LCRS cluster catalogues, respectively. A spurious detection rate of less than 5% and 1% of the EXT-FOF structures was found for the CFA1 and LCRS cluster catalogues. Both the recovery and spurious detection rates were based on the assumption that the original FOF algorithm yielded a complete structure catalogue. All of the discrepancies between the FOF and EXT-FOF group compositions were explained. We showed that our new algorithm is reluctant to identify an accumulation of galaxies as a cluster if it is very elongated along the redshift axis. This is an attribute, that makes the EXT-FOF technique very valuable for cluster-finding in photometric redshift datasets.

We furthermore tested our EXT-FOF algorithm on a dataset with simulated photometric redshifts that we created by assigning Gaussian distributed redshift offsets to the galaxies of the LCRS. A comparison of the resulting group catalogue with the one found by the EXT-FOF in case of the spectroscopic LCRS proved, that the EXT-FOF method yields a conservative cluster catalogue, and is very capable of structure finding in photometric redshift galaxy datasets. A recovery rate of almost 93% of the spectroscopic redshift structures and a spurious detection rate of about 40% of the photometric redshift structures were found. Furthermore, as was expected, a general tendency for finding larger groups was discovered in the photometric redshift case.

This paper is the first in a series of papers, dealing with the search for groups and clusters of galaxies in photometric redshift datasets. The next paper will show the application of the new EXT-FOF algorithm to the Munich Near-IR Cluster Survey (MUNICS; Drory et al. 2001b).

ACKNOWLEDGEMENTS

We want to thank Dr. John Huchra cordially for discussing his galaxy catalogue with us. Further sincere thanks go to Dr. Douglas Tucker for his extensive comments by e-mail. The MUNICS project was supported by the Deutsche Forschungsgemeinschaft, *Sonderforschungsbereich 375, Astroteilchenphysik.*

REFERENCES

Abell G. O., 1958, ApJS, 3, 211
Abell G. O., Corwin H. G., Olowin R. P., 1989, ApJS, 70, 1
Bahcall N. A., Cen R., 1992, ApJ, 398, L81
Bahcall N. A., Fan X., Cen R., 1997, ApJ, 485, L53
Baum W. A., 1962, in IAU Symp. 15: Problems of Extra-Galactic Research Vol. 15, Photoelectric Magnitudes and Red-Shifts. p. 390
Bender R., et al., 2001, in Christiani S., ed., ESO/ECF/STScI Workshop on Deep Fields "The FORS Deep Field: Photometric Data and Photometric Redshifts". Springer, Berlin, p. 327
Benítez N., 2000, ApJ, 536, 571
Bode P., Bahcall N. A., Ford E. B., Ostriker J. P., 2001, ApJ, 551, 15
Brunner R. J., Connolly A. J., Szalay A. S., 1999, ApJ, 516, 563
Carrol S. M., Press W. H., Turner E. L., 1992, ARA&A, 30, 499
Cole S., Lacey C., 1996, MNRAS, 281, 716

Couch W. J., Ellis R. S., MacLaren I., Malin D. F., 1991, MNRAS, 249, 606
Dalton G. B., Maddox S. J., Sutherland W. J., Efstathiou G., 1997, MNRAS, 289, 263
Davis M., Efstathiou G., Frenk C. S., White S. D. M., 1985, ApJ, 292, 371
de Propris R., Stanford S. A., Eisenhardt P. R., Dickinson M., Elston R., 1999, AJ, 118, 719
Drory N., Bender R., Snigula J., Feulner G., Hopp U., Maraston C., Hill G. J., de Oliveira C. M., 2001a, ApJ, 562, L111
Drory N., Feulner G., Bender R., Botzler C. S., Hopp U., Maraston C., Mendes de Oliveira C., Snigula J., 2001b, MNRAS, 325, 550
Efstathiou G., Frenk C. S., White S. D. M., Davis M., 1988, MNRAS, 235, 715
Eisenstein D. J., Hut P., 1998, ApJ, 498, 137
Eke V. R., Cole S., Frenk C. S., 1996, MNRAS, 282, 263
Fernández-Soto A., Lanzetta K. M., Yahil A., 1999, ApJ, 513, 34
Fried J. W., von Kuhlmann B., Meisenheimer K., Rix H.-W., Wolf C., Hippelein H. H., Kümmel M., Phleps S., Röser H. J., Thiering I., Maier C., 2001, A&A, 367, 788
Geller M. J., Huchra J. P., 1983, ApJS, 52, 61
Giuricin G., Marinoni C., Ceriani L., Pisani A., 2000, ApJ, 543, 178
Gladders M. D., Yee H. K. C., 2000, AJ, 120, 2148
Goto T., Sekiguchi M., Nichol R. C., Bahcall N. A., Kim R. S. J., Annis J., Ivezić Ž., Brinkmann J., Hennessy G. S., Szokoly G. P., Tucker D. L., 2002, AJ, 123, 1807
Gourgoulhon E., Chamaraux P., Fouque P., 1992, A&A, 255, 69
Heidt J., et al., 2003, A&A, 398, 49
Hopp U., Materne J., 1985, A&AS, 61, 93
Huchra J., Davis M., Latham D., Tonry J., 1983, ApJS, 52, 89
Huchra J. P., Geller M. J., 1982, ApJ, 257, 423
Jing Y., Fang L., 1994, ApJ, 432, 438
Kepner J., Fan X., Bahcall N., Gunn J., Lupton R., Xu G., 1999, ApJ, 517, 78
Kim R. S. J., Kepner J. V., Postman M., Strauss M. A., Bahcall N. A., Gunn J. E., Lupton R. H., Annis J., Nichol R. C., Castander F. J., Brinkmann J., Brunner R. J., Connolly A., Csabai I., Hindsley R. B., Ivezić Ž., Vogeley M. S., York D. G., 2002, AJ, 123, 20
Koo D. C., 1985, AJ, 90, 418
Lacey C., Cole S., 1994, MNRAS, 271, 676
Lidman C. E., Peterson B. A., 1996, AJ, 112, 2454
Lin H., Kirshner R. P., Shectman S. A., Landy S. D., Oemler A., Tucker D. L., Schechter P. L., 1996, ApJ, 464, 60
Lineweaver C. H., Tenorio L., Smoot G. F., Keegstra P., Banday A. J., Lubin P., 1996, ApJ, 470, 38
Lobo C., Iovino A., Lazzati D., Chincarini G., 2000, A&A, 360, 896
Marzke R., McCarthy P. J., Persson E., Oemler A., Dressler A., Yan M. B. L., Carlberg R., Abraham R., Ellis R., Firth A., Mackay C., McMahon R. G., 1999, in ASP Conf. Ser. 191: Photometric Redshifts and the Detection of High Redshift Galaxies The Las Campanas Infrared Survey. p. 148
Materne J., 1978, A&A, 63, 401
McCarthy P., Carlberg R., Marzke R., Chen H., Firth A., McMahon R., Wilson J., Persson E., Ellis R., Abraham R., Lahav O., Oemler A., Sabbey C., Somerville R., 2001b, in Deep Fields Clustering of Very Red Galaxies in the Las Campanas IR Survey. p. 247
McCarthy P. J., Carlberg R. G., Chen H.-W., Marzke R. O., Firth A. E., Ellis R. S., Persson S. E., McMahon R. G., Lahav O., Wilson J., Martini P., Abraham R. G., Sabbey C. N., Oemler A., Murphy D. C., Somerville R. S., Beckett M. G., Lewis J. R., MacKay C. D., 2001a, ApJ, 560, L131
Merchán M. E., Maia M. A. G., Lambas D. G., 2000, ApJ, 545, 26
Nilson P., 1973, Uppsala General Catalogue of Galaxies. Acta Universitatis Upsaliensis. Nova Acta Regiae Societatis Scientiarum Upsaliensis - Uppsala Astronomiska Observatoriums Annaler, Uppsala: Astronomiska Observatorium, 1973
Paredes S., Jones B. J. T., Martinez V. J., 1995, MNRAS, 276, 1116
Peebles P. J. E., 1993, Principles of Physical Cosmology. Princeton Series in Physics, Princeton, NJ: Princeton University Press
Plionis M., Barrow J. D., Frenk C. S., 1991, MNRAS, 249, 662
Postman M., Lubin L. M., Gunn J. E., Oke J. B., Hoessel J. G., Schneider D. P., Christensen J. A., 1996, AJ, 111, 615
Postman M., Lubin L. M., Oke J. B., 2001, AJ, 122, 1125
Press W. H., Schechter P., 1974, ApJ, 187, 425
Ramella M., Boschin W., Fadda D., Nonino M., 2001, A&A, 368, 776
Ramella M., Geller M. J., Huchra J. P., 1989, ApJ, 344, 57
Ramella M., Geller M. J., Pisani A., da Costa L. N., 2002, AJ, 123, 2976
Ramella M., Pisani A., Geller M. J., 1997, AJ, 113, 483
Schuecker P., Boehringer H., 1998, A&A, 339, 315
Shectman S. A., Landy S. D., Oemler A., Tucker D. L., Lin H., Kirshner R. P., Schechter P. L., 1996, ApJ, 470, 172
Slezak E., Bijaoui A., Mars G., 1990, A&A, 227, 301
Trasarti-Battistoni R., 1998, A&AS, 130, 341
Trentham N., 1998, MNRAS, 294, 193
Tucker D. L., Oemler A., Kirshner R. P., Lin H., Shectman S. A., Landy S. D., Schechter P. L., Muller V., Gottlober S., Einasto J., 1997, MNRAS, 285, L5
Tucker D. L., Oemler A. J., Hashimoto Y., Shectman S. A., Kirshner R. P., Lin H., Landy S. D., Schechter P. L., Allam S. S., 2000, ApJS, 130, 237
Tully R. B., 1980, ApJ, 237, 390
Tully R. B., 1987, ApJ, 321, 280
Turner E. L., Gott J. R., 1976, ApJS, 32, 409
Ueda H., Itoh M., Suto Y., 1993, ApJ, 408, 3
Valageas P., Lacey C., Schaeffer R., 2000, MNRAS, 311, 234
Williams R. E., Blacker B., Dickinson M., Dixon W. V. D., Ferguson H. C., Fruchter A. S., Giavalisco M., Gilliland R. L., Heyer I., Katsanis R., Levay Z., Lucas R. A., McElroy D. B., Petro L., Postman M., Adorf H., Hook R., 1996, AJ, 112, 1335
Williams R. E., et al., 2000, AJ, 120, 2735
Wolf C., Dye S., Kleinheinrich M., Meisenheimer K., Rix H.-W., Wisotzki L., 2001b, A&A, 377, 442
Wolf C., Meisenheimer K., Röser H.-J., Beckwith S. V. W., Chaffee F. H., Fried J., Hippelein H., Huang J.-S., Kümmel M., von Kuhlmann B., Maier C., Phleps S., Rix H.-W., Thommes E., Thompson D., 2001a, A&A, 365, 681
Zwicky F., Herzog E., Wild P., 1961-1968, Catalogue of Galaxies and of Clusters of Galaxies, 6 volumes. Pasadena: California Institute of Technology (CIT), 1961-1968
Zwicky F., Zwicky M. A., 1971, Catalogue of Selected Compact Galaxies and of Post-Eruptive Galaxies. Guemligen